Tohoku J. Exp. Med., 2018, **245**, 131-140

Hypothiocyanous Acid Suppresses PolyI:C-Induced Antiviral Responses by Modulating IRF3 Phosphorylation in Human Airway Epithelial Cells

Thuy Thu Nguyen,[1,2] Shoichi Suzuki,[1,2] Ryuichi Sugamata,[1,2] Fuyu Ito,[2] Dat Huu Tran,[1,2] Tomoko Yamamoto,[2] Shoji Kawachi[2] and Kazuo Suzuki[1,2]

[1]Department of Health Protection, Graduate School of Medicine, Teikyo University, Tokyo, Japan
[2]Asia International Institute of Infectious Disease Control, Teikyo University, Tokyo, Japan

Pattern recognition receptors recognize RNA viruses and trigger type I and III interferon (IFN) production and apoptosis to limit viral replication and spread. Some innate immune cells produce oxidants in response to viral infection to protect against invasion. Recent studies have demonstrated the virucidal activity of hypothiocyanous acid (HOSCN), an oxidant generated by the peroxidase-catalyzed reaction of thiocyanate with hydrogen peroxide. However, the effects of HOSCN on host antiviral responses are still unknown. In this study, we aimed to clarify the role of HOSCN in host antiviral responses against RNA viruses in airway epithelial cells using polyinosinic-polycytidylic acid (polyI:C), a mimic of viral RNA. Our results show that HOSCN repressed antiviral responses in NCI-H292 human airway epithelial cells. HOSCN decreased polyI:C-induced apoptosis and the expression levels of IFNB1, IFNL1, IFNL2 and IFNL3 mRNAs. In addition, the induction of other interferon regulatory factor 3 (IRF3)-dependent genes was also suppressed by HOSCN. Further analyses focused on IRF3 revealed that HOSCN inhibited the phosphorylation of IRF3 at Ser386 and Ser396 as well as its dimerization and nuclear translocation by inhibiting the phosphorylation of TANK-binding kinase 1 (TBK1). Furthermore, HOSCN led to the phosphorylation of IRF3 at residues other than Ser386 and Ser396, implying that HOSCN may cause a conformational change in IRF3 to impair its function. Collectively, these results suggest that HOSCN plays a novel signaling role in the antiviral response, acting as a negative regulator of apoptotic and TBK1-IRF3 signaling pathways and limiting IRF3-dependent gene expression.

Keywords: antiviral responses; hypothiocyanous acid; interferon regulatory factor 3; lactoperoxidase; myeloperoxidase
Tohoku J. Exp. Med., 2018 June, **245** (2), 131-140.

Introduction

The innate immune response serves as the first line of host defense against microbial infection. Pathogen-associated molecular patterns (PAMPs), which are structurally conserved microbial components, are recognized by pattern recognition receptors (PRRs), including Toll-like receptors (TLRs) and retinoic acid-inducible gene I (RIG-I)-like receptors (RLRs) (Chattopadhyay and Sen 2014). During RNA virus infection, double-stranded RNA (dsRNA) is recognized by TLR3, RIG-I, and melanoma differentiation-associated gene 5 (MDA-5) to trigger appropriate antiviral responses, including the production of various cytokines and inflammatory response factors (Akira et al. 2006). In particular, the production of type I and III interferons (IFNs; IFN-α, I FN-β and IFN-λ) induced in the early phase after viral infection is important for limiting viral replication and spread (Kawai and Akira 2006; Syedbasha and Egli 2017). In addition to type I and III IFN production, virus-infected cells undergo apoptosis in an attempt to limit the spread of the disease (Shen and Shenk 1995).

The induction of IFN genes is triggered by the activation of interferon regulatory factor 3 (IRF3) via PRRs (Akira et al. 2006). In uninfected cells, IRF3 exists as an inactive monomer in the cytoplasm. Upon viral infection, IRF3 is activated by phosphorylation at Ser386 and Ser396 by TANK-binding kinase 1 (TBK1) (Servant et al. 2003; Shu et al. 2013), leading to IRF3 dimerization and nuclear translocation and the subsequent transcription of its target genes (Shu et al. 2013; Zhao 2013). Recently, it has been demonstrated that IRF3 also functions as a key cytosolic factor for virus-induced apoptosis, although the mechanism of IRF3 activation in apoptosis differs from that of tran-

Received April 9, 2018; revised and accepted June 13, 2018. Published online June 29, 2018; doi: 10.1620/tjem.245.131.
Correspondence: Shoichi Suzuki, Department of Health Protection, Graduate School of Medicine and Asia International Institute of Infectious Disease Control, Teikyo University, 2-11-1 Kaga, Itabashi-ku, Tokyo 173-8605, Japan.
e-mail: shoichi3@med.teikyo-u.ac.jp

scriptional activation (Peters et al. 2008; Chattopadhyay et al. 2010).

Hypothiocyanous acid (HOSCN) is a microbicidal oxidant generated by the peroxidase-catalyzed reaction of thiocyanate (SCN^-) with hydrogen peroxide (H_2O_2) (Fischer 2009). In the lumen of the airway, HOSCN is generated by lactoperoxidase (LPO) secreted from the submucosal glands and surface goblet cells to eliminate invading pathogens (Fischer 2009). HOSCN is also generated by myeloperoxidase (MPO) released from neutrophils, which are recruited and activated at infectious sites (van Dalen et al. 1997; Klebanoff 2005). Some studies have demonstrated that HOSCN directly inactivates not only bacteria, but also several kinds of viruses (Mikola et al. 1995; Cegolon et al. 2014; Gingerich et al. 2016), suggesting that HOSCN has an important role against viral infection. A growing body of evidence is accumulating to show that HOSCN affects host cellular functions (Rayner et al. 2014; Chandler and Day 2015); however, there are no reports regarding the impact of HOSCN on the immune response against RNA viral infection.

In this study, in order to clarify the role of HOSCN in host antiviral responses against RNA viruses in airway epithelial cells, we examined the effect of HOSCN on the induction of apoptosis and the expression of type I and III IFNs in a human airway epithelial cell line (NCI-H292) pretreated with polyI:C, a mimic of viral RNA.

Materials and Methods

Materials

Rabbit monoclonal antibodies against IRF3, phospho-IRF3 (Ser386), and TBK1 were acquired from Abcam (Cambridge, UK), and those against phospho-IRF3 (Ser396), phospho-TBK1 (Ser172), TATA-binding protein (TBP), and beta-actin were purchased from Cell Signaling Technology (Danvers, MA, USA). Horseradish peroxidase (HRP)-linked $F(ab)_2$ fragment was purchased from GE Healthcare (Chicago, IL, USA). Lambda phosphatase was acquired from Santa Cruz Biotechnology (Santa Cruz, CA, USA), and polyinosinic-polycytidylic acid (polyI:C) was acquired from Sigma-Aldrich (St. Louis, MO, USA). Glucose oxidase (GOX) was purchased from Wako (Tokyo, Japan), and LPO was purchased from Calzyme Laboratories (San Luis Obispo, CA, USA).

Cell culture

Human lung mucoepidermoid (NCI-H292) cells were cultured in RPMI-1640 medium (Sigma-Aldrich) supplemented with 10% heat-inactivated fetal bovine serum (FBS) (HyClone, Logan, UT, USA) and 0.05 mg/ml gentamicin sulfate (Wako) at 37°C in a 5% CO_2 incubator.

Exposure of polyI:C-pretreated NCI-H292 cells to HOSCN and H_2O_2

NCI-H292 cells (2×10^6 cells in a 6-well plate or 5×10^5 cells in a 24-well plate) were stimulated with or without 20 μg/ml polyI:C in phenol red-free RPMI 1640 medium (Gibco Life Technologies, Waltham, MA, USA) containing 50 mM HEPES (pH 6.9, Wako), 3 mM NaSCN (Wako), and 5% FBS for 1 h at 37°C. After 1 h of stimulation, cells were exposed to HOSCN or H_2O_2 by adding both 16 mU/ml GOX and 10 μg/ml LPO or 16 mU/ml GOX only to the culture medium, as described previously (Suzuki et al. 2016). After 3-4 h, 250-300 μM HOSCN or 500-600 μM H_2O_2 were produced in this in vitro system. Cells were then collected for RNA isolation, protein extraction, and apoptosis assay.

Detection of apoptotic cells

NCI-H292 cells (5×10^5 cells per well in a 24-well plate) were stimulated with polyI:C for 1 h, followed by treatment with HOSCN or H_2O_2 for 4 h. At this time point, the polyI:C-pretreated cells without oxidant exposure began to show apoptotic morphological changes, but most cells were still attached to culture plates. The cells were trypsinized, washed with phosphate-buffered saline, and stained with FITC-Annexin V (FITC-AV) and ethidium homodimer III (EthD-III) according to the protocol of the Apoptotic/Necrotic/Healthy Cells Detection Kit (PromoKine, Heidelberg, Germany). Numbers of apoptotic cells were counted using the ec800™ fluorescence-activated cell sorting (FACS) system (Sony, Tokyo, Japan). Total cell number of each group was quantified by cell counting using a hemocytometer.

Isolation of RNA and quantification of mRNA expression

NCI-H292 cells (2×10^6 cells per well in a 6-well plate) were stimulated with polyI:C for 1 h, followed by treatment with HOSCN or H_2O_2 for 3 h, when polyI:C-pretreated cells showed maximal expression level of IFNB1 gene. Total RNA was isolated from cells using RNA iso Plus (Takara, Shiga, Japan), chloroform extraction, and isopropanol precipitation. cDNA was synthesized from total RNA using ReverTraAce® qPCR RT Master Mix with gDNA remover (Toyobo, Osaka, Japan). For negative control, cDNAs were prepared by excluding reverse transcriptase enzyme from the reaction mixture. Gene expression was validated by real-time PCR (qPCR) using 10 μl 2 × Power SYBR® Green PCR Master Mix (Applied Biosystems, Carlsbad, CA, USA), 5 μl cDNA (fivefold dilution), and 10 pmol specific primers for IFNB1, IFNL1, IFNL2, IFNL3, regulated on activation normal T cell expressed and secreted (RANTES), interferon gamma-induced protein 10 (IP10), interferon-stimulated gene 15 (ISG15), interferon-stimulated gene 56 (ISG56), and β-actin (as a control) (Hokkaido System Science, Hokkaido, Japan), as follows: β-actin-F:CCAACCGCGAGAAGATGA, β-actin-R:CCAGAGGCGTACAGGGATAG; IFNB1-F:CGACACTGTTCGTGTTGTCA; IFNB1-R:GAAGCACAACAGGAGAGCAA; IFNL1-F:GGGACCTGAGGCTTCTCC; IFNL1-R:CCAGGACCTTCAGCGTCA; IFNL2-F:CCTGGTGGACGTCTTGGA; IFNL2-R:GTGGGCTGAGGCTGGATA; IFNL3-F:CACACCCTGCACCATATCC; IFNL3-R:GAGCCGGTACAGCCAATG; RANTES-F:ACACCAGTGGCAAGTGCTC; RANTES-R:ACACACTTGGCGGTTCTTTC; IP10-F:GAAAGCAGTTAGCAAGGAAAGGT; IP10-R:GACATATACTCCATGTAGGGAAGTGA; ISG15-F:GCGAACTCATCTTTGCCAGTA; ISG15-R:CCAGCATCTTCACCGTCAG; ISG56-F:AGAACGGCTGCCTAATTTACAG; and ISG56-R:GCTCCAGACTATCCTTGACCTG. The qPCR cycling conditions were as follows: 95°C for 20 s, followed by 40 cycles of 95°C for 3 s and 60°C for 30 s, followed by 95°C for 15 s and 60°C for 60 s.

Protein extraction, SDS-PAGE, and immunoblotting

Whole cell extractions were prepared in RIPA lysis buffer containing 50 mM Tris-HCl (pH 7.6), 150 mM NaCl, 1 mM EDTA (pH 8.0), 1% NP-40, 1% deoxycholate, and 1 × protease inhibitor (Roche,

Basel, Switzerland), 1 mM phenylmethylsulfonyl fluoride (PMSF) (Sigma-Aldrich), and 1 × phosphatase inhibitor cocktails 2 and 3 (Sigma-Aldrich). Extraction was conducted by scraping, vortexing, sonication, and centrifugation at 20,000 × *g* at 4°C for 5 min. Cell lysates were used for SDS-PAGE and immunoblotting to detect protein expression.

Cytosolic and nuclear extracts were prepared as described previously (Schreiber et al. 1989), except that complete EDTA-free protease inhibitor cocktail and phosphatase inhibitor cocktail 2 and 3 were used in the buffers.

SDS-PAGE was performed on 7.5% acrylamide/bis gels (Bio-Rad, Hercules, CA, USA) to separate protein bands. A sample of 20 μg protein diluted in sample buffer [50 mM Tris-HCl (pH 6.8), 2% SDS, 6% glycerol, 1% 2-mercaptoethanol (Sigma-Aldrich), and 0.02% bromophenol blue] was applied to the gel and electrophoresed for 90 min at 100 V. Protein bands were transferred to a 0.2-μm Immun-Blot PVDF membrane (Bio-Rad). Blots were blocked in TBS plus 0.1% Tween-20 solution containing 3% BSA (Wako) and then incubated with 0.5 μg/ml primary antibodies, followed by incubation with HRP-linked secondary antibody. Finally, blots were developed using Pierce ECL Plus Western Blotting Substrate (Thermo-Fisher Scientific) and band intensities were measured using an Amersham Imager 600UV system (GE Healthcare).

Detection of dimerized-IRF3

Whole cell extracts were prepared as previously described (Robitaille et al. 2016) with modifications. In brief, cells were harvested by scraping. Protein was extracted in lysis buffer containing 50 mM HEPES (pH 7.4), 150 mM NaCl, 5 mM EDTA (pH 8), 1% NP-40, 10% glycerol, 1 × protease inhibitor, 1 mM PMSF, and 1 × phosphatase inhibitors via freeze/thaw in a dry ice/ethanol bath, vortexing, and centrifugation at 16,000 × *g* at 4°C for 20 min. Cell lysates were used for native PAGE, which was performed as described (Iwamura et al. 2001), except that 7.5% Mini-PROTEAN TGX precast gels (Bio-Rad) were used, and for immunoblotting with anti-IRF3 antibody to detect monomer and dimer forms of IRF3.

Treatment with phosphatase to assess IRF3 phosphorylation

Cell lysates were prepared using RIPA lysis buffer (without EDTA or phosphatase inhibitors) after 5 h of HOSCN exposure. Total protein (10 g) was treated with 400 U lambda phosphatase in lambda phosphatase buffer containing 50 mM HEPES (pH 7.5), 0.1 mM EGTA, 5 mM dithiothreitol, 0.01% BRIJ 35 and 2 mM $MnCl_2$ for 30 min at 30°C. Phosphorylation of IRF-3 was analyzed by immunoblotting with anti-IRF3 antibody

Statistical analysis

Data are presented as mean ± standard deviation (SD). Statistical analysis of results was performed using one-way ANOVA with Tukey's multiple comparison test. Differences with *p*-values < 0.05 were considered to be significant. (GraphPad Prism 7.02 software)

Results

HOSCN represses polyI:C-induced antiviral responses

First, we examined the effect of HOSCN on polyI:C-induced apoptosis. NCI-H292 cells were stimulated with polyI:C, followed by exposure to HOSCN or H_2O_2. Subsequently, the number of apoptotic cells was determined based on the cell population positive for annexin V and negative for EthD-III (upper left population in Fig. 1A-a). PolyI:C stimulation increased the cell population that was positive for Annexin V and negative for EthD-III by 25.0% (Fig. 1A-b), indicating the induction of apoptosis. HOSCN exposure decreased the population of polyI:C-induced apoptotic cells by 9.3%, restoring levels observed in control cells (7.3%) (Fig. 1A-b). In contrast, H_2O_2 treatment exhibited no effect on the induction of apoptosis (Fig. 1A-b). The double positive cell population for Annexin V and EthD-III (necrosis or secondary necrosis) showed no significant difference (Fig. 1A-c). The total number of recovered cells from each group showed no significant difference (Fig. 1A-d). These data strongly suggest that HOSCN attenuates polyI:C-induced apoptosis in NCI-H292 cells.

Next, the effect of HOSCN on the expression of IFNB1 and IFNL1-3 were analyzed. PolyI:C remarkably induced the mRNA expression of IFNB1 (468-fold), IFNL (12847-fold), IFNL2 (555-fold), and IFNL3 (1281-fold) at 4 h post-stimulation (Fig. 1B) in comparison to levels in control cells without polyI:C or oxidant stimulation. After 3 h of HOSCN exposure, the polyI:C-induced expression of these IFN genes drastically decreased, representing only a 48-fold (IFNB1), 341-fold (IFNL1), 79-fold (IFNL2), and 178-fold (IFNL3) increase over that in controls (Fig. 1B). In contrast, H_2O_2 did not decrease polyI:C-induced expression of IFNB1 (402-fold), IFNL1 (3302-fold), IFNL2 (774-fold), and IFNL3 (1592-fold) at 3 h post-H_2O_2 exposure (Fig. 1B). Thus, HOSCN attenuated the polyI:C-induced expression of the cytokine genes IFNB1, IFNL1, IFNL2, and IFNL3 in NCI-H292 cells. These results strongly suggest that HOSCN represses antiviral responses, including the induction of apoptosis and the expression of the IFNB1 and IFNL1-3 mRNAs.

HOSCN represses polyI:C-induced expression of IRF3 target genes

In the antiviral response, both apoptosis and expression of IFNB1 and IFNL1-3 mRNA are reportedly regulated by IRF3; therefore, we examined the impact of HOSCN on the expression of other IRF3-dependent genes in polyI:C-pretreated cells. After 4 h of stimulation, polyI:C drastically induced the mRNA expression of RANTES (100-fold increase), IP10 (922-fold increase), ISG15 (35-fold increase), and ISG56 (36-fold increase) (Fig. 2). HOSCN exposure markedly attenuated the polyI:C-induced upregulation of RANTES (25-fold), IP10 (107-fold), ISG15 (11-fold), and ISG56 (9-fold), while H_2O_2 only slightly reduced the mRNA expression of RANTES (73-fold), IP10 (673-fold), ISG15 (31-fold), and ISG56 (28-fold) (Fig. 2). Thus, HOSCN exposure attenuated the polyI:C-induced expression of these IRF3-regulated genes more effectively than H_2O_2. We hypothesized that the reductions in the expression of these genes were associated with the HOSCN-induced suppression of IRF3 activation.

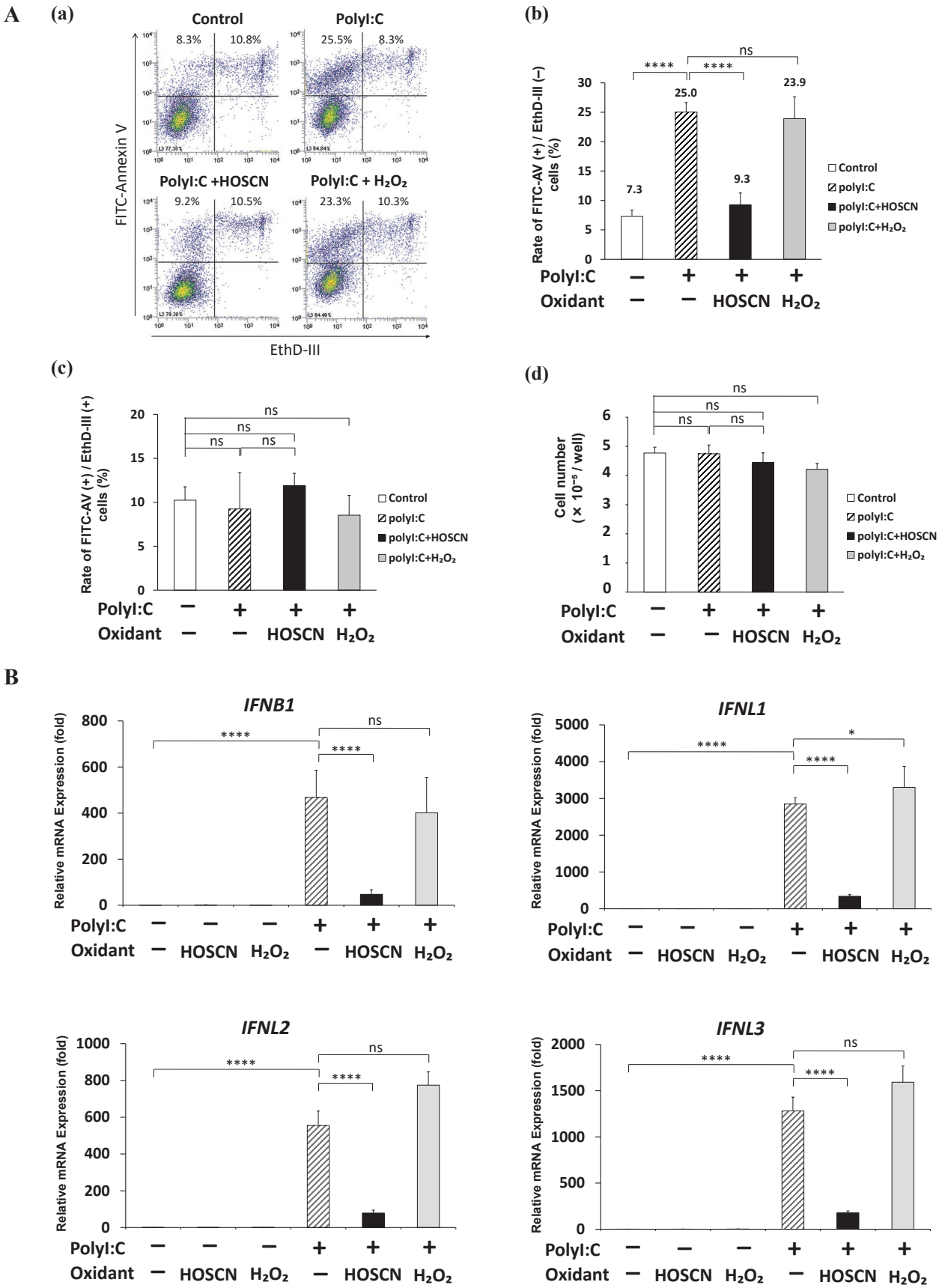
A
(a)
Control
PolyI:C
8.3%
10.8%
25.5%
8.3%
PolyI:C +HOSCN
PolyI:C + H2O2
9.2%
10.5%
23.3%
10.3%
FITC-Annexin V
EthD-III
(b)
Rate of FITC-AV (+) / EthD-III (–) cells (%)
****
****
ns
7.3
25.0
9.3
23.9
Control
polyI:C
polyI:C+HOSCN
polyI:C+H2O2
PolyI:C
Oxidant
HOSCN
H2O2
(c)
Rate of FITC-AV (+) / EthD-III (+) cells (%)
ns
(d)
Cell number (× 10−5 / well)
B
IFNB1
IFNL1
IFNL2
IFNL3
Relative mRNA Expression (fold)

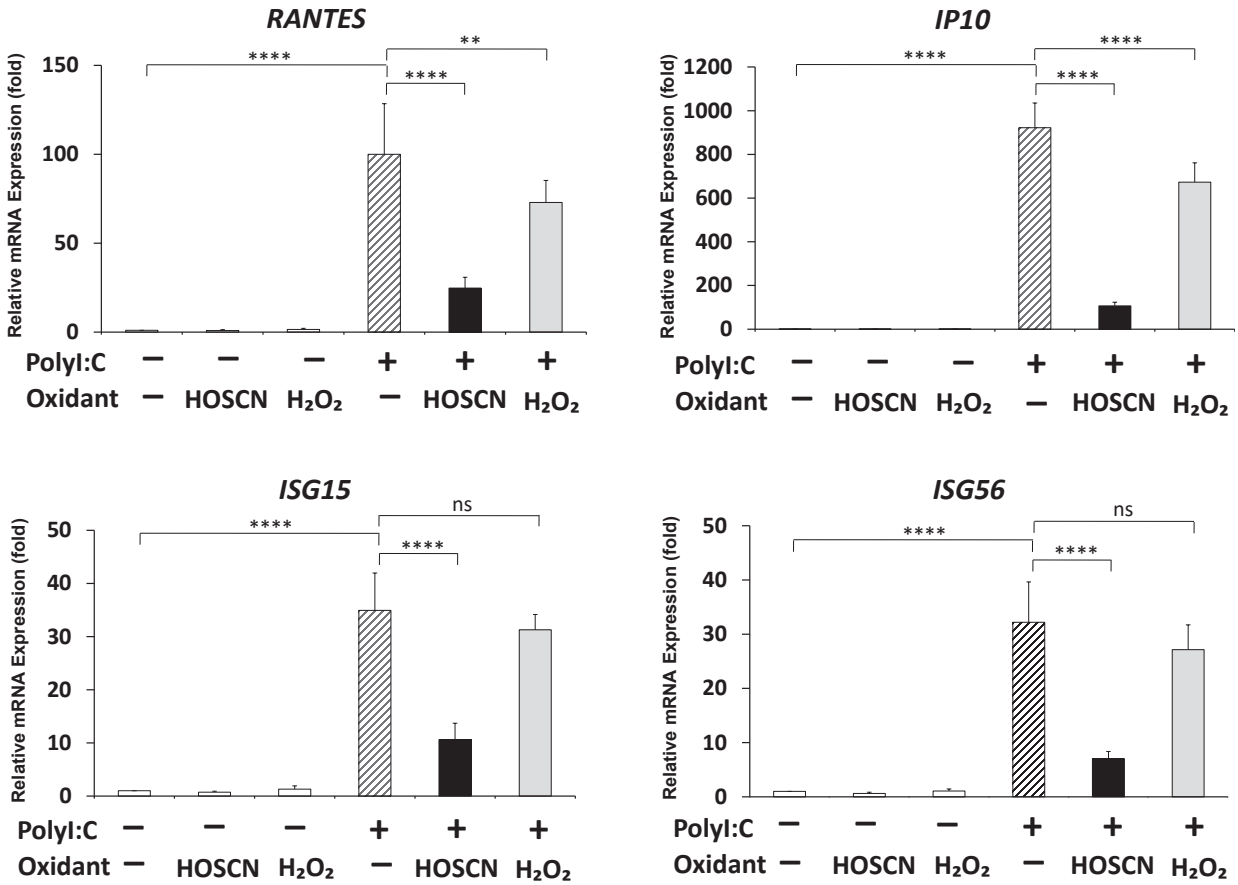

Fig. 2. HOSCN attenuated polyI:C-induced expression of IRF3 target genes.
Cells were stimulated with polyI:C (striped) for 1 h or untreated, and then exposed to HOSCN (black) or H_2O_2 (light grey) for 3 h. RNA was extracted, and the expression levels of RANTES, IP10, ISG15, and ISG56 mRNAs were analyzed by qRT-PCR. Data were normalized with β-actin and are presented as mean ± SD of three independent experiments. One-way ANOVA with Tukey's multiple comparison test was used for statistical analysis.
****$p < 0.0001$, **$p < 0.01$.
ns, not significant.

HOSCN inhibits the dimer formation of IRF3 by repressing its phosphorylation via TBK1

To determine the mechanism by which HOSCN attenuates the polyI:C-induced mRNA expression of IRF3-regulated genes, we analyzed the effect of HOSCN on the dimerization of IRF3 using native-PAGE and immunoblotting with an anti-IRF3 antibody. As shown in Fig. 3A, polyI:C induced the dimer formation of IRF3. In contrast, HOSCN attenuated the polyI:C-induced dimerization of IRF3, while the dimerization of IRF3 was not affected by H_2O_2 treatment (Fig. 3A).

The phosphorylation of IRF3 at Ser386 and Ser396 has been shown to be an essential regulator of IRF3 dimer formation (Chen et al. 2008; Takahasi et al. 2010); therefore, we examined the effect of HOSCN on the phosphorylation of IRF3 at Ser386 and Ser396 by immunoblotting

Fig. 1. HOSCN attenuated polyI:C-induced antiviral responses.
(A) HOSCN attenuated polyI:C-induced apoptosis. NCI-H292 cells were stimulated with or without polyI:C for 1 h, followed by exposure to HOSCN or H_2O_2 for 4 h. (a) Cells were stained with FITC-AV and EthD-III for FACS analysis to count the percentage of apoptotic cells (representative of four experiments). The rates of FITC-AV (+) /EthD-III (–) cells and FITC-AV (+) /EthD-III (+) cells in each group was shown in (b) and (c), respectively. (d) Cell number of each group were quantified using a hemocytometer. (B) HOSCN attenuated polyI:C-induced expression of IFNB1, IFNL1, IFNL2, and IFNL3 mRNAs. Cells were stimulated with polyI:C (striped) for 1 h or untreated, followed by exposure to HOSCN (black) or H_2O_2 (light grey) for 3 h. RNA was extracted, and the expression levels of IFNB1, IFNL1, IFNL2, and IFNL3 mRNAs were analyzed by qRT-PCR. Data were normalized with β-actin and are presented as mean ± SD of three independent experiments. One-way ANOVA with Tukey's multiple comparison test was used for statistical analysis.
****$p < 0.0001$, *$p < 0.05$.
ns, not significant.

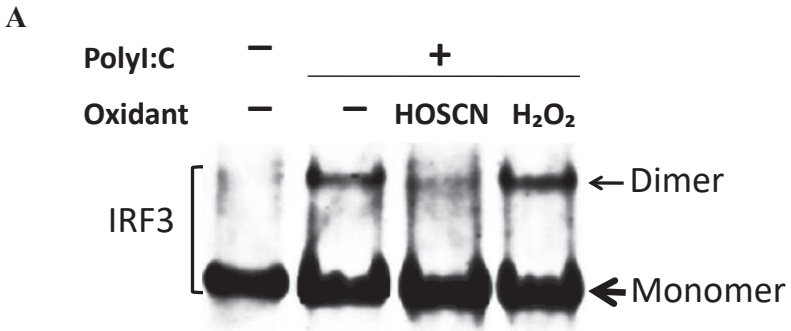
A
PolyI:C
Oxidant
HOSCN
H2O2
IRF3
Dimer
Monomer

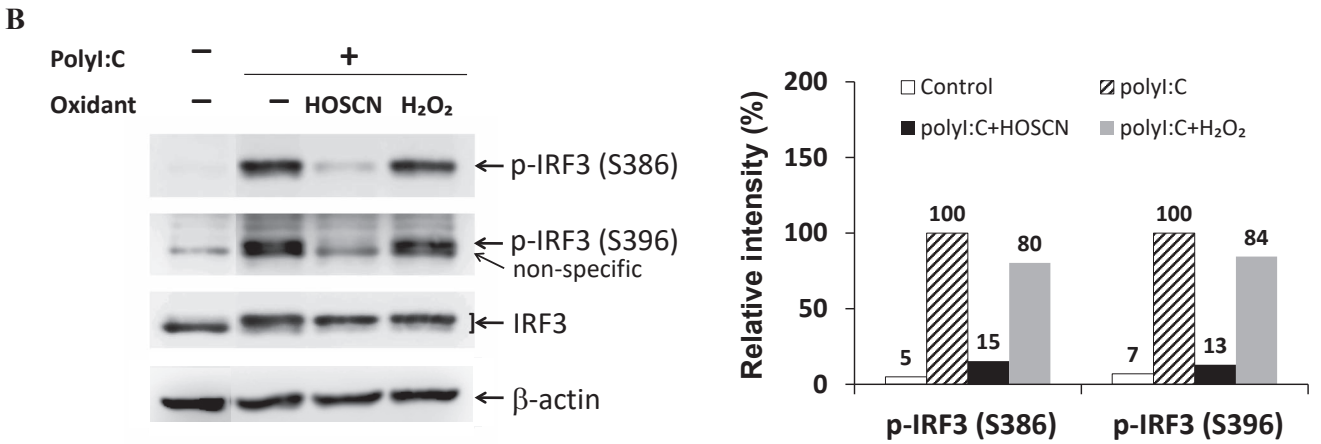
B
PolyI:C
Oxidant
HOSCN
H2O2
p-IRF3 (S386)
p-IRF3 (S396)
non-specific
IRF3
β-actin
Control
polyI:C
polyI:C+HOSCN
polyI:C+H2O2
Relative intensity (%)
200
150
100
50
0
5
100
15
80
7
100
13
84
p-IRF3 (S386)
p-IRF3 (S396)

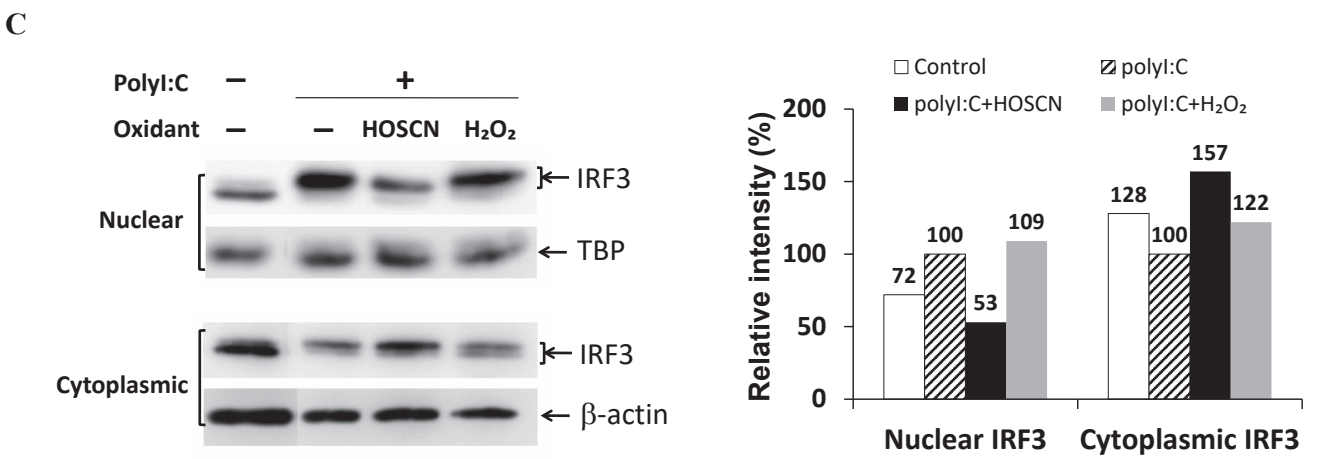
C
PolyI:C
Oxidant
HOSCN
H2O2
Nuclear
IRF3
TBP
Cytoplasmic
IRF3
β-actin
Control
polyI:C
polyI:C+HOSCN
polyI:C+H2O2
Relative intensity (%)
200
150
100
50
0
72
100
53
109
128
100
157
122
Nuclear IRF3
Cytoplasmic IRF3

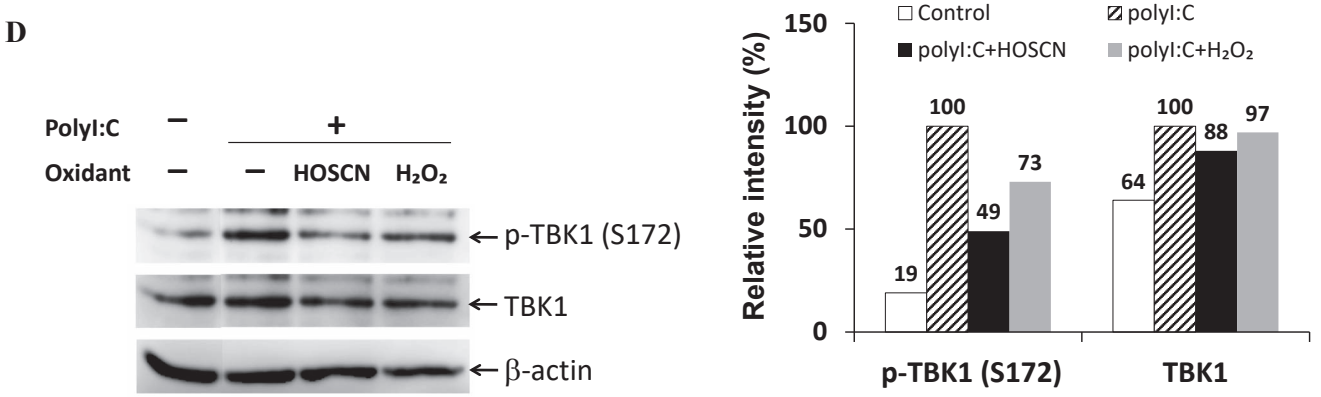
D
PolyI:C
Oxidant
HOSCN
H2O2
p-TBK1 (S172)
TBK1
β-actin
Control
polyI:C
polyI:C+HOSCN
polyI:C+H2O2
Relative intensity (%)
150
100
50
0
19
100
49
73
64
100
88
97
p-TBK1 (S172)
TBK1

with p-IRF3 (Ser386) and p-IRF3 (Ser396). We found that the polyI:C-induced phosphorylation of IRF3 at Ser386 and Ser396 was suppressed by HOSCN, but not by H_2O_2 (Fig. 3B).

The effect of HOSCN on the translocation of IRF3 into the nucleus was next considered, as it is the dimerized-IRF3 form that translocates into the nucleus and binds to the promoters of IRF3 target genes. The immunoblotting of nuclear extracts with anti-IRF3 antibody demonstrated that polyI:C stimulation increased the amount of nuclear IRF3 (Fig. 3C). HOSCN treatment reduced the amount of IRF3 in the nucleus, whereas H_2O_2 had no effect on the translocation of IRF3. Inversely, the amount of IRF3 in the cytoplasmic extract was considerably increased following HOSCN treatment (Fig. 3C). These results indicate that HOSCN inhibits the translocation of IRF3 into the nucleus.

We next examined whether the inhibitory effect of HOSCN on IRF3 activation involves TBK1 phosphorylation, as IRF3 activation is mediated by the phosphorylation of TBK1. As shown in Fig. 3D, polyI:C stimulation increased the phosphorylation of TBK1 at Ser172, but this polyI:C-induced increase in the phosphorylation of TBK1 was attenuated after exposure to HOSCN and H_2O_2 for 3 h. Moreover, HOSCN attenuated the phosphorylation of TBK1 more strongly than H_2O_2. These data suggest that HOSCN inhibits the phosphorylation of TBK1, resulting in the inhibition of IRF3 activation.

HOSCN phosphorylates IRF3 at amino acid residues other than Ser386 and Ser396

Finally, we used SDS-PAGE to examine whether HOSCN exposure without polyI:C pretreatment affects the phosphorylation status of IRF3, as a recent study suggested that the phosphorylation of IRF3 at the residues other than Ser386 and Ser396 impairs its activation (Meng et al. 2016).

Compared to controls without polyI:C or oxidants, a more slowly migrating band was observed for IRF3 when cells were exposed to HOSCN, but this was not observed for H_2O_2 (Fig. 4A). The slower band was not detected by phosphorylation-dependent antibodies of IRF3, suggesting that HOSCN may induce phosphorylation at amino acid residues other than Ser386 and Ser396. We confirmed that the migration delay observed with SDS-PAGE was due to the phosphorylation of IRF3 using phosphatase (Fig. 4B). After phosphatase treatment, the IRF3 band migrated more rapidly than before phosphatase treatment. This result clearly shows that HOSCN induces IRF3 phosphorylation at amino acid residues other than Ser386 and Ser396. HOSCN-induced phosphorylation was observed at 1 h post-HOSCN exposure (Fig. 4C), indicating a rapid response to HOSCN. These results suggest that the HOSCN-induced phosphorylation of IRF3 may be related to impairment of IRF3 activation following HOSCN treatment.

Discussion

In this study, we demonstrated that HOSCN attenuates polyI:C-induced apoptosis and expression of IFNB1 and IFNLs mRNAs in airway epithelial cells. In addition, HOSCN down-regulates the expression levels of IRF3-dependent genes, such as *RANTES*, *IP10*, *ISG15*, and *ISG56,* which are upregulated by polyI:C. These results indicate that HOSCN suppresses the antiviral response in airway epithelial cells. We also showed that HOSCN negatively controls IRF3 activation by inhibiting TBK1 phosphorylation. Regarding the inhibitory mechanisms of HOSCN, we speculate that TBK1 activity may be directly or indirectly repressed by a hypothetical factor that is activated in response to oxidative stress induced by HOSCN. One such candidate is protein kinase A (PKA). A previous study has shown that HOSCN promotes PKA regulatory subunits to homodimerize via disulfide bonds, thus activating its catalytic subunits in a cyclic adenosine monophosphate-independent manner (Suzuki et al. 2016). Recently, it has been found that PKA activation leads to the degradation of interferon-beta promoter stimulator-1 (Yan et al. 2017), which is a key molecule in the RIG-I-TBK1-IRF3 signaling axis involved in TBK1 activation. Another candidate is mammalian sterile 20-like kinase 1 (MST1), which is known to be activated by cellular oxidative stress through distinct pathways involving thioredoxin-1 (Chae et al. 2012) and peroxiredoxin-1 (Morinaka et al. 2011). Recently, MST1 has been identified as a negative regulator of TBK1 during viral infection (Meng et al. 2016).

We also observed that HOSCN exposure induces the phosphorylation of IRF3 at amino acid residues other than Ser386 and Ser396. It is thus possible that IRF3 phosphorylation at these residues inhibits dimer formation and the

Fig. 3. HOSCN inhibited the dimer formation of IRF3 by suppressing its phosphorylation via TBK1.
(A) HOSCN inhibited polyI:C-induced dimerization of IRF3. NCI-H292 cells were stimulated with polyI:C for 1 h or untreated, then exposed to HOSCN or H_2O_2 for 3 h. Cell lysates were used to detect IRF3 dimerization using native PAGE and immunoblotting with anti-IRF3 antibody. The thin arrow indicates the dimer form of IRF3, and the large arrow indicates the monomer form of IRF3. (B) HOSCN inhibited the phosphorylation of IRF3 at Ser386 and Ser396. NCI-H292 cells were stimulated with polyI:C for 1 h or untreated, then exposed to HOSCN or H_2O_2 for 3 h. Cell lysates were prepared and analyzed by SDS-PAGE and immunoblotting with antibodies against IRF3, p-IRF3 (Ser386), and p-IRF3 (Ser396). (C, D) HOSCN inhibited the translocation of IRF3 into the nucleus (C) and the phosphorylation of TBK1 (D). Cells were stimulated with polyI:C for 1 h or untreated, then exposed to HOSCN or H_2O_2 for 3 h. Cell lysates were prepared and analyzed by SDS-PAGE and immunoblotting with antibodies against IRF3, TBK1, and p-TBK1 (Ser172). The band intensities were measured and normalized with TBP or β-actin. Data were expressed as percentage values relative to the level of polyI:C-stimulated cells without oxidant exposure set at 100. All experiments were performed at least more than two times.

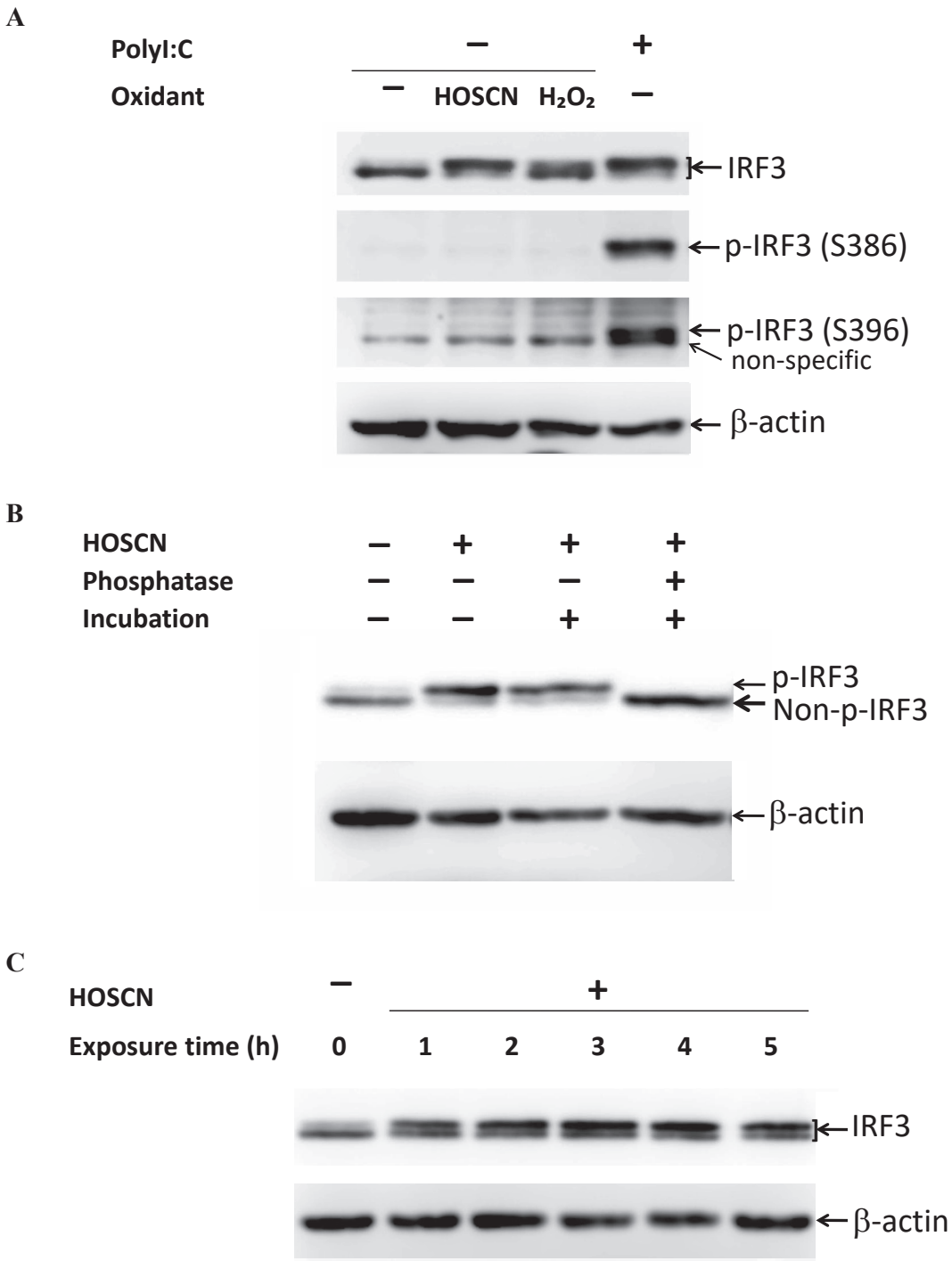

Fig. 4. HOSCN phosphorylated IRF3 at amino acid residues other than Ser386 and Ser396.
(A) HOSCN induced phosphorylation of IRF3 at distinct residues. NCI-H292 cells were stimulated with polyI:C for 1 h or untreated, then exposed to HOSCN or H_2O_2 for 3 h. Cell lysates were prepared and analyzed by SDS-PAGE and immunoblotting with antibodies against IRF3, p-IRF3 (Ser386), and p-IRF3 (Ser396). (B) De-phosphorylated IRF3. Cells were exposed to HOSCN for 5 h or untreated. Cell lysates were then treated with phosphatase or untreated at 30°C for 30 min. The phosphorylation of IRF3 was analyzed by immunoblotting with anti-IRF3 antibody. The thin arrow indicates phosphorylated IRF3, and the large arrow indicates non-phosphorylated IRF3. (C) Time course-dependent phosphorylation of IRF3. Cells were exposed to HOSCN for 1-5 h or untreated. Cell lysates were analyzed with IRF3 activation assay using SDS-PAGE and immunoblotting with anti-IRF3 antibody. All experiments were performed three times independently.

DNA binding activity of IRF3. In fact, it has been suggested that the phosphorylation of IRF3 at the Thr75 and Thr253 residues leads to the inhibition of DNA binding and dimer formation, respectively (Meng et al. 2016).

We further observed that HOSCN suppresses polyI:C-induced apoptosis, though the mechanisms by which this occurs are still unknown. Recently, a new apoptosis pathway mediated by IRF3 and activated during viral infection has been discovered. In this pathway, IRF3 is activated by the linear ubiquitination of its lysine residues, which triggers its interaction with B-cell lymphoma 2-associated X protein (BAX), leading to mitochondrial activation and apoptosis (Chattopadhyay et al. 2016). It has been reported that lysine residues can be carbamylated with cyanate (Wang et al. 2007), a decomposition product of HOSCN (Kalmár et al. 2011). Therefore, it is possible that HOSCN inhibits the interaction of IRF3 with BAX by blocking the ubiquitination of IRF3 lysine residues. In addition, the new apoptosis pathway mediated by IRF3 is shown to be caspase-dependent (Chattopadhyay et al. 2016). HOSCN has been reported to inhibit caspase 3 activation via oxidation of its active site in human umbilical vein endothelial cells (Bozonet et al. 2010). Therefore, it is possible that HOSCN suppresses polyI:C-induced apoptosis by inhibiting caspase 3 activity in airway epithelial cells.

The next question is, what is the biological significance of our finding that HOSCN represses antiviral responses? In airway epithelial cells, the major sources of H_2O_2 are thought to be dual oxidase (DUOX) 1 and 2 (Geiszt et al. 2003). Recent studies have shown that DUOX2 is induced in cells in the late phase after virus infection (Fink et al. 2013), suggesting that higher levels of HOSCN may be generated by the DUOX/LPO system in the late phase. If so, HOSCN may have an important role in terminating antiviral responses to avoid host damage. Even in the early phase after viral infection, HOSCN may be produced by the Nicotinamide adenine dinucleotide phosphate oxidase 2/MPO system in a SCN^- concentration dependent manner in the case of viral infections associated with neutrophil infiltration. In this situation, higher levels of HOSCN may accelerate viral replication and spread, resulting in severe disease outcomes. Interestingly, SCN^- concentrations in the plasma are 2-5 times higher in smokers than in non-smokers (Spagnolo et al. 1988; Wang et al. 2007), owing to the detoxification of hydrogen cyanide in cigarette smoke (Spagnolo et al. 1988). This suggests that elevated levels of HOSCN may be generated in smokers. Therefore, our observations indicate that in smokers, HOSCN may accelerate viral replication and spread, leading to severe disease outcomes. In fact, there are many reports that cigarette smoking exacerbates viral infectious diseases (Arcavi and Benowitz 2004).

In conclusion, our study results suggest that HOSCN plays a novel signaling role in the antiviral response, acting as a negative regulator of apoptotic and TBK1-IRF3 signaling pathways and limiting IRF3-dependent gene expression.

Acknowledgments

This study was supported by the Japanese Government Scholarship Monbukagakusho (MEXT), e-ASIA Joint Research Program, Japan Agency for Medical Research and Development (AMED) (No. Jp16jm0210032), Japan Science and Technology Agency (JST), Grant-in-aid for scientific research from the Japan Society for the Promotion of Science (No. 17K08792) and Vietnam Ministry of Science and Technology (MOST). In addition, we thank Dr. Thuy Phung Thi Bich at the Vietnam National Children's Hospital for her valuable discussion. We also thank Editage (www.editage.jp) for English language editing.

Conflict of Interest

The authors declare no conflict of interest.

References

Akira, S., Uematsu, S. & Takeuchi, O. (2006) Pathogen recognition and innate immunity. *Cell*, **124**, 783-801.

Arcavi, L. & Benowitz, N.L. (2004) Cigarette smoking and infection. *Arch. Intern. Med.*, **164**, 2206-2216.

Bozonet, S.M., Scott-Thomas, A.P., Nagy, P. & Vissers, M.C. (2010) Hypothiocyanous acid is a potent inhibitor of apoptosis and caspase 3 activation in endothelial cells. *Free Radic. Biol. Med.*, **49**, 1054-1063.

Cegolon, L., Salata, C., Piccoli, E., Juarez, V., Palu', G., Mastrangelo, G. & Calistri, A. (2014) In vitro antiviral activity of hypothiocyanite against A/H1N1/2009 pandemic influenza virus. *Int. J. Hyg. Environ. Health*, **217**, 17-22.

Chae, J.S., Gil Hwang, S., Lim, D.S. & Choi, E.J. (2012) Thioredoxin-1 functions as a molecular switch regulating the oxidative stress-induced activation of MST1. *Free Radic. Biol. Med.*, **53**, 2335-2343.

Chandler, J.D. & Day, B.J. (2015) Biochemical mechanisms and therapeutic potential of pseudohalide thiocyanate in human health. *Free Radic. Res.*, **49**, 695-710.

Chattopadhyay, S., Kuzmanovic, T., Zhang, Y., Wetzel, J.L. & Sen, G.C. (2016) Ubiquitination of the transcription factor IRF-3 activates RIPA, the apoptotic pathway that protects mice from viral pathogenesis. *Immunity*, **44**, 1151-1161.

Chattopadhyay, S., Marques, J.T., Yamashita, M., Peters, K.L., Smith, K., Desai, A., Williams, B.R. & Sen, G.C. (2010) Viral apoptosis is induced by IRF-3-mediated activation of Bax. *EMBO J.*, **29**, 1762-1773.

Chattopadhyay, S. & Sen, G.C. (2014) dsRNA-activation of TLR3 and RLR signaling: gene induction-dependent and independent effects. *J. Interferon Cytokine Res.*, **34**, 427-436.

Chen, W., Srinath, H., Lam, S.S., Schiffer, C.A., Royer, W.E. & Lin, K. (2008) Contribution of Ser386 and Ser396 to activation of interferon regulatory factor 3. *J. Mol. Biol.*, **379**, 251-260.

Fink, K., Martin, L., Mukawera, E., Chartier, S., De Deken, X., Brochiero, E., Miot, F. & Grandvaux, N. (2013) IFNβ/TNFα synergism induces a non-canonical STAT2/IRF9-dependent pathway triggering a novel DUOX2 NADPH oxidase-mediated airway antiviral response. *Cell Res.*, **23**, 673-690.

Fischer, H. (2009) Mechanisms and function of DUOX in epithelia of the lung. *Antioxid. Redox Signal.*, **11**, 2453-2465.

Geiszt, M., Witta, J., Baffi, J., Lekstrom, K. & Leto, T.L. (2003) Dual oxidases represent novel hydrogen peroxide sources supporting mucosal surface host defense. *FASEB J.*, **17**, 1502-1504.

Gingerich, A., Pang, L., Hanson, J., Dlugolenski, D., Streich, R., Lafontaine, E.R., Nagy, T., Tripp, R.A. & Rada, B. (2016) Hypothiocyanite produced by human and rat respiratory epithelial cells inactivates extracellular H1N2 influenza A virus. *Inflamm. Res.*, **65**, 71-80.

Iwamura, T., Yoneyama, M., Yamaguchi, K., Suhara, W., Mori, W., Shiota, K., Okabe, Y., Namiki, H. & Fujita, T. (2001) Induction of IRF-3/-7 kinase and NF-kappaB in response to double-stranded RNA and virus infection: common and unique pathways. *Genes Cells*, **6**, 375-388.

Kalmár, J., Woldegiorgis, K.L., Biri, B. & Ashby, M.T. (2011) Mechanism of decomposition of the human defense factor hypothiocyanite near physiological pH. *J. Am. Chem. Soc.*, **133**, 19911-19921.

Kawai, T. & Akira, S. (2006) Innate immune recognition of viral infection. *Nat. Immunol.*, **7**, 131-137.

Klebanoff, S.J. (2005) Myeloperoxidase: friend and foe. *J. Leukoc. Biol.*, **77**, 598-625.

Meng, F., Zhou, R., Wu, S., Zhang, Q., Jin, Q., Zhou, Y., Plouffe, S.W., Liu, S., Song, H., Xia, Z., Zhao, B., Ye, S., Feng, X.H., Guan, K.L., Zou, J., et al. (2016) Mst1 shuts off cytosolic antiviral defense through IRF3 phosphorylation. *Genes Dev.*, **30**, 1086-1100.

Mikola, H., Waris, M. & Tenovuo, J. (1995) Inhibition of herpes simplex virus type 1, respiratory syncytial virus and echovirus type 11 by peroxidase-generated hypothiocyanite. *Antiviral. Res.*, **26**, 161-171.

Morinaka, A., Funato, Y., Uesugi, K. & Miki, H. (2011) Oligomeric peroxiredoxin-I is an essential intermediate for p53 to activate MST1 kinase and apoptosis. *Oncogene*, **30**, 4208-4218.

Peters, K., Chattopadhyay, S. & Sen, G.C. (2008) IRF-3 activation by Sendai virus infection is required for cellular apoptosis and avoidance of persistence. *J. Virol.*, **82**, 3500-3508.

Rayner, B.S., Love, D.T. & Hawkins, C.L. (2014) Comparative reactivity of myeloperoxidase-derived oxidants with mammalian cells. *Free Radic. Biol. Med.*, **71**, 240-255.

Robitaille, A.C., Mariani, M.K., Fortin, A. & Grandvaux, N. (2016) A high resolution method to monitor phosphorylation-dependent activation of IRF3. *J. Vis. Exp.*, e53723.

Schreiber, E., Matthias, P., Müller, M.M. & Schaffner, W. (1989) Rapid detection of octamer binding proteins with 'mini-extracts', prepared from a small number of cells. *Nucleic Acids Res.*, **17**, 6419.

Servant, M.J., Grandvaux, N., tenOever, B.R., Duguay, D., Lin, R. & Hiscott, J. (2003) Identification of the minimal phosphoacceptor site required for in vivo activation of interferon regulatory factor 3 in response to virus and double-stranded RNA. *J. Biol. Chem.*, **278**, 9441-9447.

Shen, Y. & Shenk, T.E. (1995) Viruses and apoptosis. *Curr. Opin. Genet. Dev.*, **5**, 105-111.

Shu, C., Sankaran, B., Chaton, C.T., Herr, A.B., Mishra, A., Peng, J. & Li, P. (2013) Structural insights into the functions of TBK1 in innate antimicrobial immunity. *Structure*, **21**, 1137-1148.

Spagnolo, A., Torsello, S., Morisi, G., Petrozzi, E., Antonini, R., Ricci, G., Urbinati, G.C. & Menotti, A. (1988) Serum thiocyanate levels as an objective measure of smoking habits in epidemiological studies. *Eur. J. Epidemiol.*, **4**, 206-211.

Suzuki, S., Ogawa, M., Ohta, S., Nunomura, S., Nanri, Y., Shiraishi, H., Mitamura, Y., Yoshihara, T., Lee, J.J. & Izuhara, K. (2016) Induction of airway allergic inflammation by hypothiocyanite via epithelial cells. *J. Biol. Chem.*, **291**, 27219-27227.

Syedbasha, M. & Egli, A. (2017) Interferon lamda: modulating immunity in infectious diseases. *Front. Immunol.*, **8**, 119.

Takahasi, K., Horiuchi, M., Fujii, K., Nakamura, S., Noda, N.N., Yoneyama, M., Fujita, T. & Inagaki, F. (2010) Ser386 phosphorylation of transcription factor IRF-3 induces dimerization and association with CBP/p300 without overall conformational change. *Genes Cells*, **15**, 901-910.

van Dalen, C.J., Whitehouse, M.W., Winterbourn, C.C. & Kettle, A.J. (1997) Thiocyanate and chloride as competing substrates for myeloperoxidase. *Biochem. J.*, **327**, 487-492.

Wang, Z., Nicholls, S.J., Rodriguez, E.R., Kummu, O., Hörkkö, S., Barnard, J., Reynolds, W.F., Topol, E.J., DiDonato, J.A. & Hazen, S.L. (2007) Protein carbamylation links inflammation, smoking, uremia and atherogenesis. *Nat. Med.*, **13**, 1176-1184.

Yan, B.R., Zhou, L., Hu, M.M., Li, M., Lin, H., Yang, Y., Wang, Y.Y. & Shu, H.B. (2017) PKACs attenuate innate antiviral response by phosphorylating VISA and priming it for MARCH5-mediated degradation. *PLoS Pathog.*, **13**, e1006648.

Zhao, W. (2013) Negative regulation of TBK1-mediated antiviral immunity. *FEBS Lett.*, **587**, 542-548.